Case Studies in Thermal Engineering 49 (2023) 103276

Contents lists available at ScienceDirect

Case Studies in Thermal Engineering

journal homepage: www.elsevier.com/locate/csite

Solar-assisted hybrid oil heating system for heavy refinery products storage

Naseer Ahmad Khan [a], Asif Hussain Khoja [a,*], Naveed Ahmed [a,b,**], Fahid Riaz [c,***], Mariam Mahmood [a], Majid Ali [a], M.A. Kalam [d], M.A. Mujtaba [e]

[a] Department of Thermal Energy Engineering, U.S.-Pakistan Centre for Advanced Studies in Energy (USPCAS-E), National University of Sciences & Technology (NUST), Sector H-12, Islamabad, 44000, Pakistan
[b] Department of Energy and Petroleum Engineering, Universitet I Stavanger, 4021, Stavanger, Norway
[c] Mechanical Engineering Department, Abu Dhabi University, Abu Dhabi, P.O. Box 59911, United Arab Emirates
[d] School of Civil and Environmental Engineering, University of Technology Sydney, Ultimo, NSW, Australia
[e] Department of Mechanical Engineering, University of Engineering and Technology (New Campus), Lahore, 54890, Pakistan

GRAPHICAL ABSTRACT

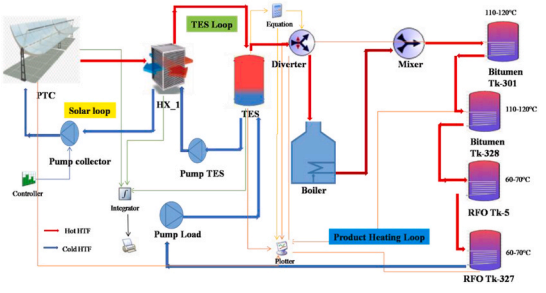

ARTICLE INFO

Keywords:
Oil refinery
Parabolic trough collector
Thermal energy storage
GHG mitigation
Economic feasibility
Solar fraction

ABSTRACT

The purpose of this study is to investigate the potential use of solar energy within an oil refinery to reduce its fossil fuel consumption and greenhouse gas emissions. A validated ASPEN HYSYS model was used to investigate the products produced from heavy crude oil in the refinery. Using TRNSYS software, the proposed Parabolic Trough Collector (PTC)-based solar heating system paired with the boiler is modelled. Sensible thermal energy storage (TES) system is integrated into the refinery's process heating to handle the intermittent nature of solar energy. It was discovered

* Corresponding author.
** Corresponding author. Department of Thermal Energy Engineering, U.S.-Pakistan Centre for Advanced Studies in Energy (USPCAS-E), National University of Sciences & Technology (NUST), Sector H-12, Islamabad, 44000, Pakistan.
*** Corresponding author. Mechanical Engineering Department, Abu Dhabi University, Abu Dhabi, P.O. Box 59911, United Arab Emirates.
E-mail addresses: asif@uspcase.nust.edu.pk (A. Hussain Khoja), naveed.ahmed@uspcase.nust.edu.pk (N. Ahmed), fahid.riaz@adu.ac.ae (F. Riaz).

https://doi.org/10.1016/j.csite.2023.103276
Received 1 March 2023; Received in revised form 21 May 2023; Accepted 8 July 2023
Available online 16 July 2023

that 463 m^2 of the PTC area coupled with a 15000-L TES tank can result in a maximum life cycle cost savings of 21.046 thousand USD for an annual heat supply of 116,944 MWh to generate steam at a temperature of 200–220 °C. In the proposed hybrid heating system, the yearly solar fraction is determined to be 26.99% and the payback period is 8.77 years with the average solar irradiance of 900 W/m^2. In addition, the system can yearly reduce greenhouse gas (GHG) emissions by about 34.045 tonnes of CO_2 equivalents.

Abbreviations and symbols:

ARL	Attock Refinery Limited
GHGs	Greenhouse gases
TES	Thermal energy storage
SIPH	Solar industrial process heat
LPG	Liquefied Petroleum Gas
HCU	Heavy Crude Unit
BPD	barrel per day
CPT	Crude Preheat Train
A	Area[m^2]
T	Temperature [°C]
ΔT	Change in temperature [°C]
Q	Heat transfer rate (KJ/h)
P	Power of pump [W]
C_P	Specific Heat Capacity [kJ/kg K]
HC_E	Heavy crude exchanger
TCR	Top circulating reflux
MCR	Medium circulating reflux
LCR	Lower circulating reflux
PTC	Parabolic trough collector
DNI	Direct Normal Irradiance
HX	Heat Exchanger
HC_V_1	Heavy crude atmospheric distillation tower
HC_V_5	Heavy crude vacuum distillation tower
LDO	Light Diesel Oil
HSD	High-Speed Diesel
RFO	Residual Fuel Oil
HVGO	Heavy Vacuum Gas Oil
LVGO	Light Vacuum Gas Oil
PA	Pump around
HC_H	Heavy Crude Heater
HC_C	Heavy Crude Cooler
JBO	Jute Batching Oil
HTF	Heat transfer fluid
Tk	Tank
P	Pass
RD	Rundown

Subscript

Env	Environment
In	In let
Out	Outlet
I	Initial
F	Final
Min	Minimum
Aux	Auxiliary
η_{hth}	heater efficiency

1. Introduction

Oil refining is an energy-intensive process that needs a large amount of direct or indirect heat [1]. Particularly, about 32–35% of the entire global energy is consumed in the industrial sectors [2]. Burning fossil fuels to generate process steam for industrial uses results in the release of GHGs, which contribute to global warming [3]. The worldwide search for alternative fuels continues due to the ongoing depletion of conventional fuels [4,5]. The technology of producing steam using solar energy has been researched all around the world [6], with the majority of studies focusing on concentrated solar collectors such as PTC [7]. The bulk of industrial processes, such as pasteurization, extraction, dehydration, sterilization, and distillation, operate at the medium temperature range between 60 °C and 280 °C. For this temperature range, it is essential to investigate the viability of using renewable energy sources, such as solar energy, to provide low-pressure process steam for industrial sectors [8,9].

Due to the intermittent nature of solar resources, there is a mismatch between energy supply and demand. Concentrating solar power (CSP) linked with TES can play a major role in the transition to a sustainable energy system because thermal energy can be stored in a TES for steam generation at night-time or in unfavorable conditions [10]. In a TES, the energy is stored as sensible heat, latent heat, or a combination of both sensible and latent heat [11]. The thermal energy is stored in sensible heat storage by rising the temperature of the storage material [12]. The phase change material is used in the latent heat storage system to store thermal energy by changing its phase [13]. Solar thermal systems integrating with TES make the system efficient and provide operational flexibility [14, 15].

In recent times, numerous studies have been done to examine the viability of solar industrial process heat (SIPH) for various applications. In various regions of India, Sharma et al. [16] examined the potential of SIPH and its environmental advantages in the dairy business. They calculated that SIPH could supply 6.4 PJ/year of useable energy in the Indian dairy industry; SIPH might also provide 4.50 PJ of useful energy if the process heating need is limited to the pasteurization stage of milk processing. They discovered that using SIPH in the dairy business could reduce 32–144 thousand tonnes of CO_2. Baniassadi et al. [17] proposed a new concept that can assist in the design and operation of solar heat-integrated systems with heat storage. They discovered that 17% of the system's

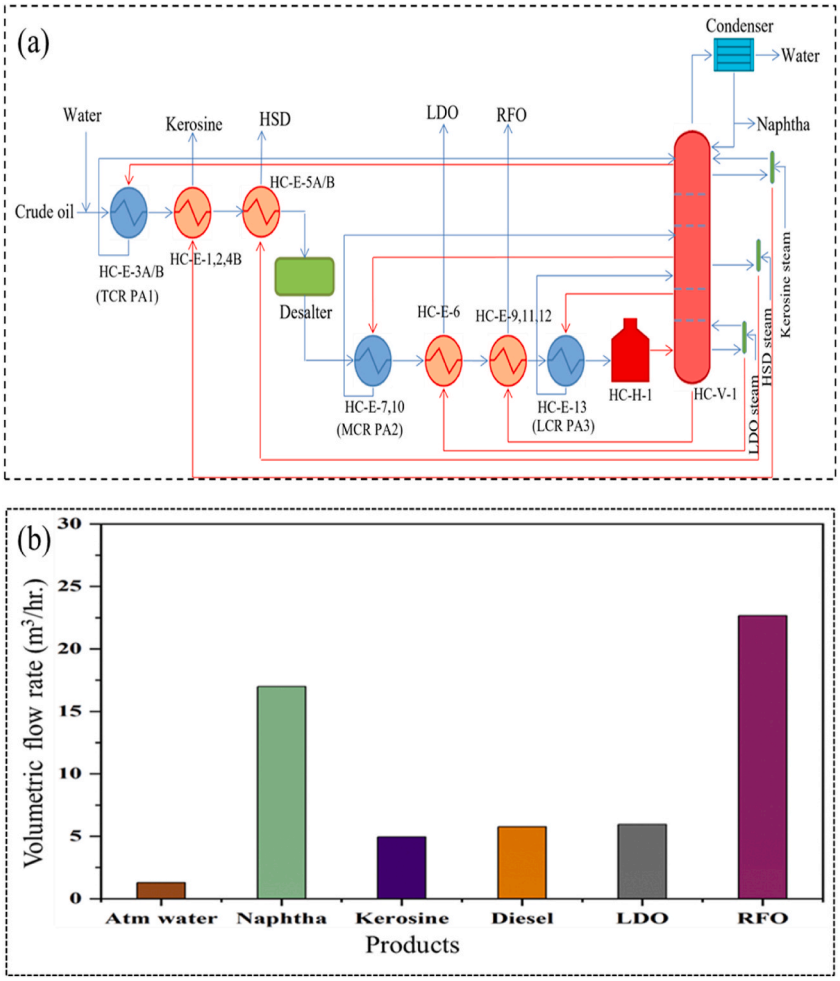

Fig. 1. (a) Crude oil process flow diagram (b) Products produced through an atmospheric distillation tower.

energy is derived from the sun using 1000 collectors. With 6000 collectors, however, the system's solar contribution was enhanced by up to 47%. The results also reveal that without heat storage, the maximum solar fraction for 6000 collectors is 20%. 6000 collectors achieved a solar fraction of 27% when heat storage was incorporated with the system. The case study assesses the impact of storage size, heat loss rate, minimum solar temperature difference, collector area, and efficiency on the solar fraction.

Allouhi et al. [18] conducted a case study at a Moroccan milk processing plant situated in Casablanca, and the life cycle cost approach was used to determine the appropriate size of the primary design elements for decision-making. For an annual heat requirement of 528.23 MWh, it was discovered that 400 m^2 of Evacuated tube solar collectors slanted at a 30° angle linked with a 2000 L TES tank can result in a maximum life cycle cost savings of 179 thousand USD. The entire yearly solar fraction is found to be 41% in this ideal design, 12.27 years is the payback period. The technology can cut greenhouse gas emissions by 77.23 tonnes of CO_2 equivalents per year. Mokhtari Shahdost et al. [19] evaluated the technological and economic viability of preheating process fluid with solar energy before it enters refinery furnaces. Compared to the range of temperature of the process fluid heated by furnaces, which is approximately 300 °C, solar energy at moderate temperature is a feasible energy source. Solar energy can provide a maximum of 23.77% of the furnace's annual energy consumption in optimal conditions. This reduces the amount of fuel consumed by the furnace by up to 1,996,000 cubic metres per year and prevents the release of 3557.7 tonnes of carbon dioxide. Altayib and Dincer [20] examine a unique thermal configuration for an industrial heating process. A thermal storage system (TES) is included to handle the sun's intermittent nature. The system's energy and exergy efficiencies were determined to be 60.94 and 19.34%, respectively. In addition, a 10% solar contribution to crude oil heating reduces 11,950 tonnes of CO_2 annually. These investigations demonstrate that the utilization of solar thermal energy using a parabolic trough collector is one of the most efficient methods.

After the careful literature survey, it is concluded that most of the studies have focused on preheating of process fluid in different industries with conventional heating systems. However, to the best of the author's knowledge, no work has been reported for steam generation using the proposed solar hybrid system by maintaining the temperature of the refinery products in the storage tank. The purpose of this study is to evaluate the proposed hybrid heating system for heavier refinery products in the storage tank, coupled with TES. Moreover, the study presents energy analysis, cost analysis, and GHG emission analysis of the proposed solar hybrid system in oil refinery.

2. Methodology

2.1. Process design and description of the refinery

The heating of process fluid in refineries is done with oil-fired fuel heaters. Sustainable and environmentally beneficial heating methods, such as solar energy are needed to augment traditional heating systems. In the current work, the preliminary data is collected from the Heavy Crude Unit (HCU) in Attock Refinery Limited (ARL) Rawalpindi, Pakistan. The HCU plant has an installed capacity of 8500 barrels per day (BPD) or (56.36 m^3/h) and uses a mixture of light and heavy crude oil to operate. The HCU in ARL is a fully integrated two–stage crude distillation unit. Through a network of heat exchangers known as a crude preheat train (CPT), 60–70% of the desired thermal energy is supplied by hot streams from the distillation tower [21]. The boosted heavy crude flows into the first pre-heat train and is heated by-products or intermediate products or pump-around refluxes from the Heavy Crude Atmospheric distillation tower (HC–V-1) and Heavy Crude Vacuum distillation tower (HC–V-5). The crude is heated to 90–120 °C and then flows to

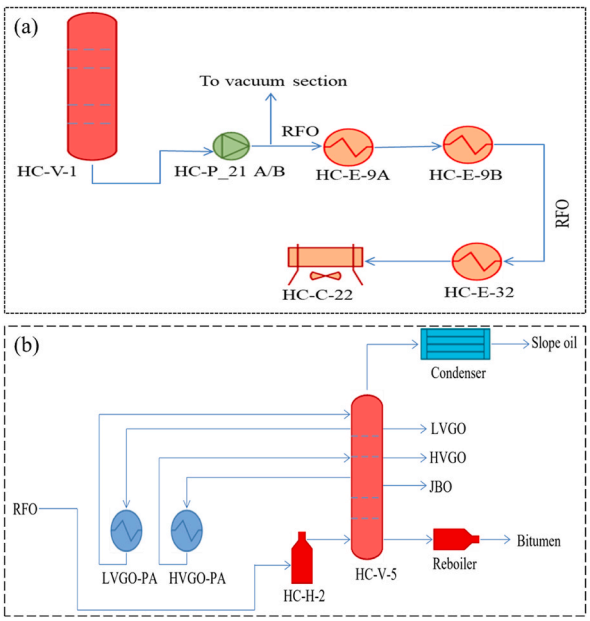

Fig. 2. (a) The bottom product drawn off through fractionator (b) Crude oil flow to vacuum tower.

the desalting section as shown in Fig. 1(a). By first pre-heat train the crude oil flow through the tube side of the Heavy crude heat exchanger (HC-E) after passing through each heat exchanger, crude oil gains heat from heated products or pump around refluxes. The temperature and pressure of the products before and after passing through the heat exchanger are shown in Table S1.

In crude oil refining, desalting is a crucial step before distillation. Depending on the source of crude oil, different amounts and types of salts may be present [22]. A typical purchase specification specifies a maximum salt content of around 4.5 kg per thousand barrels, which may require oil desalting at refineries [23]. The desalted heavy crude is heated by the products or intermediate products or pump-around refluxes from HC-V-1 and HC-V-5 in the heat exchangers at the second pre-heat train. By this preheating crude oil is heated to 180–210 °C and then flows to Heavy Crude Atmospheric Charge Heater (HC–H-1) as shown in Fig. 1(a). The temperature and pressure of the products before and after passing through the heat exchanger at the second pre-heat train are shown in Table S1. Crude is further heated to 320–340 °C after passing through the HC-H-1. At HCU, the atmospheric distillation column is installed with 42 Trays and crude oil feed enters the 37th Tray (Flash Zone) in the HC-V-1. In the atmospheric distillation column, the products are separated on the base of the boiling point. Low boiling point products go to the top trays and high ones go to the bottom trays. Volumetric flow rates of the products produced through the atmospheric distillation column are shown in Fig. 1(b).

The products at the bottom of the Fractionator are drawn off and boosted by Fractionator Bottom Pump (HC–P-21 A/B) and transferred to the Vacuum Section as shown in Fig. 2(a). A part of the bottom is split at the discharge line of the Fractionator Bottom Pump. The split stream is cooled in Feed/RFO Heat Exchanger (HC-E−9A/B), RFO Heat Exchanger (HC-E−32), and RFO Fin-Fan Cooler (HC-E−22) and sent to the storage tank.

The bottom of the Heavy Crude Fractionator is heated with a Heavy Crude Vacuum Charge Heater (HC–H-2) to 360–400 °C. The partially vaporized bottoms from HC-V-1 enter the flash zone of HC-V-5, as shown in Fig. 2(b), which has 14 theoretical plates with packing beds. The volumetric flow rate of the products produced through the vacuum tower are as follows:

- Slope oil (0.939 m^3/h)
- LVGO (0.890 m^3/h)
- HVGO (1.436 m^3/h)
- JBO (0.299 m^3/h)
- Bitumen (1.423 m^3/h)

The products of atmospheric and vacuum distillation towers are stored in individuals' storage tanks. The storage temperature of the products produced through the atmospheric and vacuum distillation tower is shown in Table 1. The two products Residual Fuel Oil (RFO) and Bitumen stored in the storage tank which passes the coil to maintain its temperature. In Table S2 Tk-307 and Tk-05 shows the product storing capacity of the tank of RFO and presently stock available and the ullage of products to fill the tank, while Tk-301 and Tk-328 show the product storing capacity of the tank of Bitumen and presently stock available and the ullage of products to fill the tank of bitumen.

2.2. Solar integrated hybrid process design

The software TRNSYS has been used for both thermodynamic modelling and economic analysis. Fig. 3 depicts the modelling of the solar energy transfer and conventional heat transfer as well as the TRNSYS variables. The main components of the operating system include PTC, variable speed pump, pipe, heat exchanger, TES, diverter, mixer, Boiler, and Energy demand system or Crude oil Product Storage Tank.

2.2.1. Solar loop and weather data

The solar loop involves PTC, variable speed pump, pipes, and heat exchanger as shown in Fig. S1. PTC having a 463 m^2 area. Antifreeze solution Therminol VP-1 oil serves as the heat-carrying medium in the collectors. The properties of Therminol VP-1 are shown in Table 2. The output temperature of the heat transfer fluid (HTF) (i.e., the temperature of the fluid at the exit of collectors) is dependent on solar field size and ambient conditions. The system comprises pipes to transport the heated solution to the TES loop where its heat is transferred to sunflower oil through a heat exchanger (HX-1) and heated sunflower oil is used to charge TES. The inside diameter of the pipe is 50 mm at which HTF flows through the solar loop. Valenzuela et al. [24], determined that the flow rate of the HTF per one row of solar collectors ranges between 0.35 and 0.80 kg/s. This range is designed for a non-looping single collector row. This study considers a total mass flow rate of 15 kg/s entering and exiting the solar field.

In a solar field, the weather is one of the influencing elements. For entering weather data, type 15-3 epw file is used. The net irradiation for the refinery's geographical position on the horizontal surface over a year (8760 h) has been obtained using the TRNSYS software. Direct Normal Irradiance (DNI) is considered to be the input parameter in the modelling of PTC. The range of DNI is relatively broad and does not fluctuate substantially throughout the year. Its discrepancy is primarily attributable to overcast days during the

Table 1
Products storage temperature.

Products	Storage temp	Products	Storage temp
NAPHTHA	38 °C	RFO	66 °C
KEROSINE	35 °C	Slope oil	35 °C
HSD	60 °C	JBO	66 °C
LDO	55 °C	Bitumen	121 °C

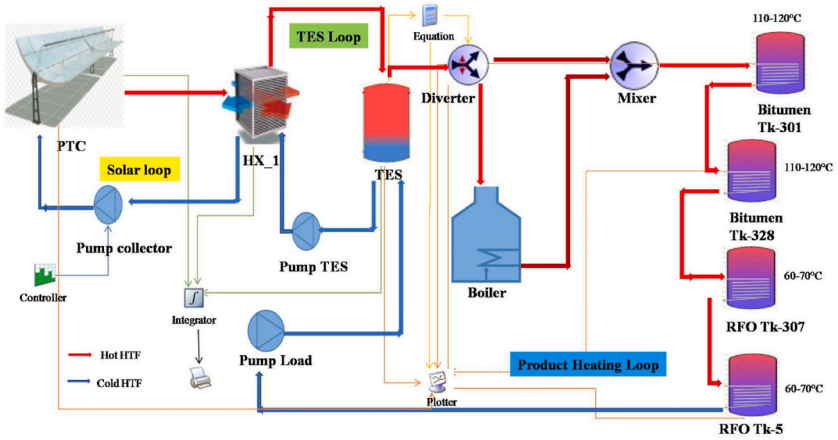

Fig. 3. Process flow diagram of solar integration with boiler.

Table 2
Properties of Therminol VP-1 oil [25].

Property	Value	Unit
Specific heat	2.45793	kJ/kg K
Density	764.293	kg/m^3
Operating temperature	285.15–673.15	K
Thermal capacity	1872.517	kJ/K m^3

humid months of the year. As shown in Fig. S2(a), the total irradiance on a horizontal surface varies significantly throughout the year based on the direction of solar irradiation. According to the weather data for location of Rawalpindi, the average sunlight duration is calculated to be 12 h each day, and the average solar irradiance is 900 W/m^2.

The ambient temperature and wind speed in the area are two additional aspects that have an impact on the efficiency of the solar field. Fig. S2(b) illustrates the variations in ambient temperature and wind speed that occurred at various times throughout the year. The range of the ambient temperature is 5–45 °C. According to Fig. S2(b), the highest wind velocity is 13 m/s (46.8 km/h) and this has no effect on the operation of the collector.

2.2.2. Parabolic trough collector integration

Depending on the type of thermal collector, solar thermal collectors are utilized to collect solar energy and transport it as heat to a thermal network. CSP can use significantly hotter working fluids than non-concentrating solar systems. HTF oils such as Therminol VP-1 can be used in concentrated solar systems to function at temperatures as high as 400 °C [26]. In this simulation, the PTC (Type 1245) from the standard TES thermal solar collector library has been selected. Without sun tracking, the PTC (Type 1245) is able to achieve moderate concentration. The absorber and HTF are enclosed in an evacuated glass tube behind an exterior reflecting concentrator. The end-user can regulate the HTF flow rate through the collector to maintain the outlet temperature [27]. PTC collectors were used having the total aperture area of 463 m^2. The efficiency of the collector is computed using the Hottel-Whillier steady-state condition equation, which is then simplified to the following Eqs. (1) and (2) [28];

$$\eta = a_0 - a_1\frac{(\Delta T)}{I_T} - a_2\frac{(\Delta T)^2}{I_T} \tag{1}$$

$$\eta = \frac{Q_{\text{useful}}}{\text{A } I_T} \tag{2}$$

Eq. (1) is the general collector efficiency equation, where a_0, a_1, and a_2 are the thermal efficiency parameters available for collectors evaluated in accordance with American Society of Heating, Refrigerating, and Air-Conditioning Engineers (ASHRAE) standards and rated by Solar Rating & Certification Corporation (SRCC) [28], in addition to solar collectors evaluated in accordance with the most

Table 3
The thermal collector's technical specifications.

Parameter	Value	Unit
a_0	0.75	[−]
a_1	0.27	[−]
a_2	0	[−]

recent European Standards (CEN,2001). The useful energy gain for solar collectors can be obtained using Eq. (2), where A is the collector's area [m^2] and I_T refers to the incidence of solar irradiation [W/m^2] on collectors. The technical specification of solar thermal collector is shown in Table 3.

The Type110 is a model of a variable speed pump that can sustain a certain outlet mass flow rate between zero and a rated value. The setting of the control signal causes a linear variation in the mass flow rate of the pump. The forcing function is modelled with component Type 14, for transient simulation, it is useful to employ a time-dependent forcing function. A series of discrete data points that indicate the value of the function at various intervals throughout one cycle are used to define the pattern of the forcing function. This pattern is then used to determine how the function will behave throughout the cycle.

Using Eq. (3) (Adapted from TRNSYS Library), to calculate the energy transferred from the pump motor to the fluid stream.

$$\dot{Q}_{fluid} = P_{shaft}\left(1-\eta_{pumping}\right) + \left(\dot{P}-\dot{P}_{shaft}\right) f_{motorless} \tag{3}$$

where $\eta_{pumping}$ is the efficiency of the pump, P_{shaft} is shaft power and $f_{motorless}$ is the fraction of pump motor.

Energy transferred from the pump motor to ambient air is calculated by Eq. (4) (Adapted from TRNSYS Library).

$$\dot{Q}_{ambient} = \left(\dot{P}-\dot{P}_{shaft}\right)\left(1-f_{motorless}\right) \tag{4}$$

The temperature of the fluid exiting the pump can be expressed by Eq. (5) (Adapted from TRNSYS Library).

$$T_{fluid,out} = T_{fluid,in} + \frac{\dot{Q}_{fluid}}{\dot{m}_{fluid}} \tag{5}$$

where $T_{fluid,\ in}$ is the temperature of the fluid inlet to pump, Q_{fluid} is the energy transferred to the fluid and m_{fluid} is the mass flow rate.

Pipe is modelled with component Type 31. The exit of the pipe is a collection of elements that are pushed out by the incoming flow. The rate of overall energy loss to the environment is the sum of each element loss and can be expressed by Eq. (6) [29].

$$\dot{Q}_{env,\ j} = (UA)_j\ \left(T_j - T_{env}\right) \tag{6}$$

where $Q_{env,\ j}$ is the heat loss rate to segments of fluid in a pipe, U is the coefficient of heat loss, A is the actual area in which the loss has been discovered, T_j temperature of the segment of fluid in the pipe, and T_{env} represents pipe environment temperature.

Using Eq. (7) (Adapted from TRNSYS Library), the change in the internal energy of the fluid in a pipe is determined.

$$\Delta E = mC_p\ \left(T_f - T_i\right) \tag{7}$$

Heat exchanger (Type 761) is modelled to have the capability of maintaining the temperature difference between the cold side inlet and outlet, it is controlled by using Eq. (8) [30].

$$T_{cold,out} = T_{cold,in} + \frac{\dot{Q}_{HX}}{C_{coldside}} \tag{8}$$

$\dot{Q}_{HX}$ is the rate of heat transfer across the heat exchanger, which can be determined with Eq. (9) [31].

$$\dot{Q}_{HX} = \varepsilon C_{min}\left(T_{hot,in} - T_{cold,in}\right) \tag{9}$$

Where epsilon (ε) represents the efficiency of the heat exchanger and C_{min} represents the minimum of the fluid thermal capacitances on both the hot and cold sides that are used between the solar and TES loops.

2.2.3. Thermal energy storage loop

The TES loop contains the TES tank with a volume of 15 m^3 and a variable speed pump as shown in Fig. S3. As both the solar loop and the product heating loop are connected to the TES loop, it serves as the central hub of the entire system. The HTF contained in the TES loop is sunflower oil. The properties of sunflower HTF are shown in Table S3 [32]. Allouhi et al. [33] presented similar concepts for energy storage, however, the proposed design differs in that it has two TES exits. The first exit of sunflower oil is at the bottom after the exchange of thermal energy to TES. The second exit of steam at the top after gaining thermal energy from TES. During the daytime when the sun is available, the TES loop is used to charge the TES tank.

Dowtherm A medium is used in the TES system. It is the eutectic mixture of two very stable compounds biphenyl ($C_{12}H_{10}$); diphenyl oxide ($C_{12}H_{10}O$). The Dowtherm A (which is a eutectic combination) tank is charged with sunflower oil that absorbs heat from the solar loop HTF. Utilizing a centralized storage tank, extra thermal energy is stored and utilized during cloudy days and at night. Through HX-1 the solar thermal energy captured by PTC transfers to sunflower oil HTF of the TES loop. Collector and TES pumps are connected to circulate and sustain the fluid flow through the Parabolic trough collector and sides of the TES tank. During the day, the system is directly powered by solar energy, while at night; the steam is produced by the heat energy stored in the Dowtherm A at the TES tank. The properties of Dowtherm A are given in Table S4 [34].

2.2.4. Product heating loop

The product heating loop involves pump, pipe, diverter, mixer, boiler, and product storage tank as shown in Fig. S4. HTF used in this loop is steam. Pump pumped the steam to the TES tank where this loop is used to discharge the TES. The steam exit at the top of TES

and flows toward the diverter. By the controller, outlet1, and outlet 2 of the diverter are controlled. When the temperature of the steam is equal to or greater than 180 °C, outlet 1 of the diverter is open and at the same time, outlet 2 is closed. Through outlet 1, the steam directly flows toward the product storage tank. But when the temperature of the steam is less than 180 °C, then outlet 1 is closed and outlet 2 is open, and steam flow toward the boiler where fossil fuel burns to raise the temperature of a fluid to 210–230 °C.

Firing device or hot water boiler with Type 659 controlled by Eq. (10) [35].

$$\dot{Q}_{aux} = \frac{\dot{m}C_p(T_{out} - T_{in}) - UA(T_{ave} - T_{amb})}{\eta_{htr}} \tag{10a}$$

Here η_{htr} is the heater efficiency.

The system utilized a pipe to carry steam toward the product storage tank to maintain the temperature of bitumen and RFO at the storage tank.

2.3. Validation procedure

In this section, Fig. 4 represents the comparison of simulation results of heavy crude oil products storage temperature obtained from TRNSYS software with the actual data acquired from the refinery industry to validate the proposed system. From the figure, it can be observed that the simulation model's results coincide well with the actual measured data. Actual data was taken from a refinery where Bitumen was stored at 120-110 °C and RFO was stored at 70-60 °C. The simulated outcome falls within this range.

3. Results and discussion

The daily and annual heating demand for RFO and bitumen products are presented in the current study. The presented analysis of solar hybrid is based on maintaining the required temperature of refinery products before dispatch from the product storage tank. Due to the intermittent behaviour of solar energy, the solar field is integrated with TES. Understanding the thermodynamic operation of a solar hybrid heating system to generate steam, TRNSYS software is used to simulate a solar field with a 463 m^2 PTC area for two days, a sunny day (1st January), and a partially cloudy day (7th February).

3.1. Thermal performance analysis on sunny days

The solar field input and output temperatures as well as the DNI and total radiation on a horizontal surface throughout 24 h on a sunny day are represented in Fig. 5(a). As shown in the figure, DNI is more uniform than the total radiation on a sunny day. The temperature of the HTF as it leaves the solar field is essentially unaltered during sunny periods since PTC only reflects the DNI onto the absorbing pipe. Additionally, the outlet temperature is directly proportional to DNI.

HTF from the solar loop will transfer heat to HTF of the TES loop through a HX_1. Type761 models a heat exchanger have the capability of maintaining the temperature difference between the cold side inlet and outlet. Solar loop fluid flow through the hot side of

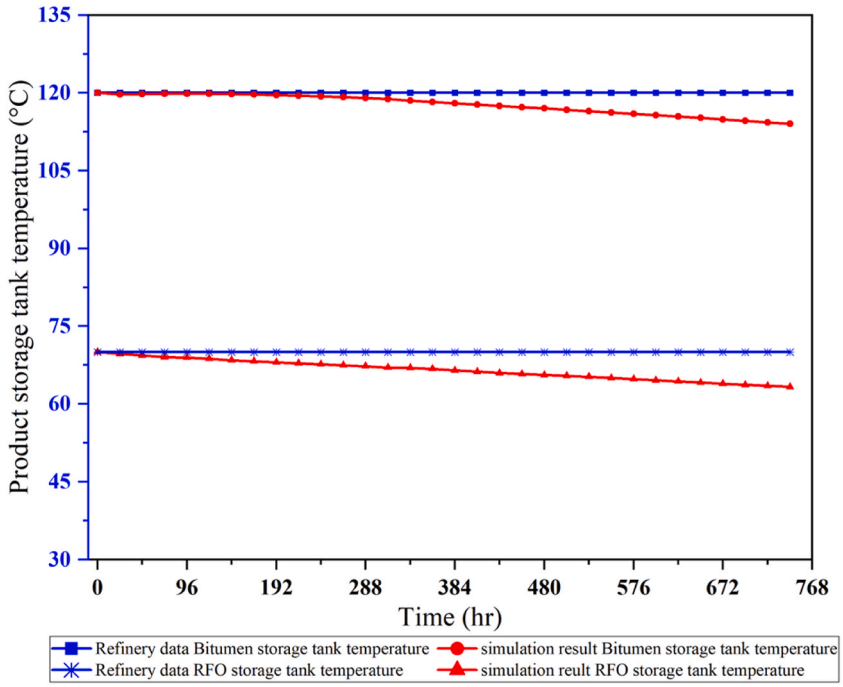

Fig. 4. Product storage temperature_ comparing refinery data and simulation result.

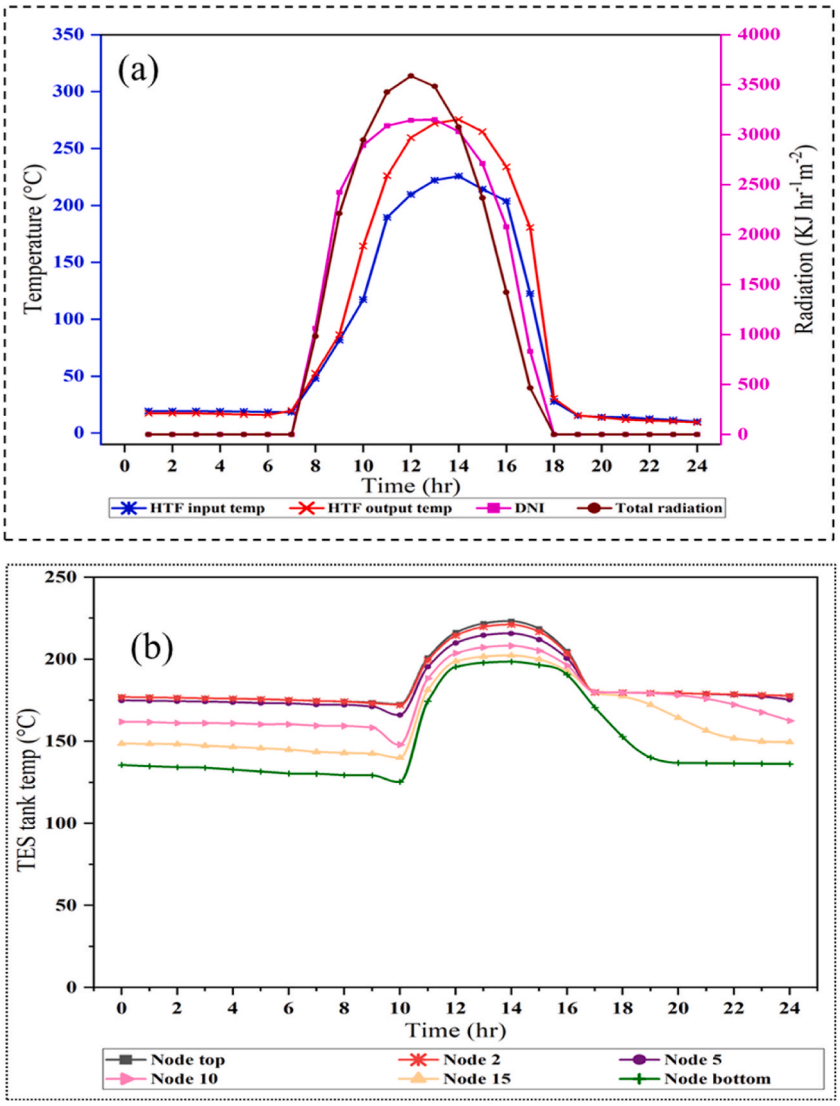

Fig. 5. (a) Temperature of the solar collector input and output, total radiation on horizontal surface and DNI, on a sunny day (b) TES tank node temperature, on a sunny day.

the HX-1 and TES loop fluid flow through the cold side of the HX-1. The flow rate of the cold-side fluid exiting the heat exchanger enters TES. The fluid will enter the storage tank at the node closest in temperature to the cold side outlet temperature. An equal flow rate of the fluid leaves the bottom of the thermal storage tank for return to the HX_1.

Fig. 5(b) shows the temperature of the specified node of the TES tank. TES height (5.35 m) is divided into 20 nodes, starting from node 01 at the top to node 20 at the bottom of tank. All the nodes are equally distributed along the TES height with 0.28 m gap between nodes. As shown in the diagram, the temperature at the top node of the TES tank at the beginning of the day is 175 °C, at noon time temperature increases up to 220 °C due to presence of the solar energy, while at night the temperature drops to 180 °C due to non-availability of solar energy. The temperature at the bottom node of the thermal energy storage tank is lower than at the top node because in the charging cycle of the TES tank, HTF from the heat source side inlet to TES tank at the top and exits at the bottom of the tank.

Fig. 6(a) shows the temperature of the steam inlet to TES, the outlet from TES and the boiler, and the outlet flow rate from the diverter. As shown in the diagram the steam inlet to the TES tank at the temperature of 140–150 °C. The steam gains thermal energy from TES (discharging the cycle of the TES tank) and exit at a temperature higher than the inlet of steam. After gaining thermal energy the steam flows toward the diverter. Through controller, the diverter outlet is controlled. When the temperature of the steam is equal to or higher than 180 °C, outlet 1 of the diverter is open and outlet 2 is closed. From outlet 1 of the diverter the steam flow toward inlet 1 of the mixer and proceeds to the product storage tank to maintain the temperature of products before despatch from the storage tank (Tk) in the refinery. After maintaining the temperature of products i.e., bitumen at Tk-301, Tk-328, and RFO at Tk-307, Tk-05 the

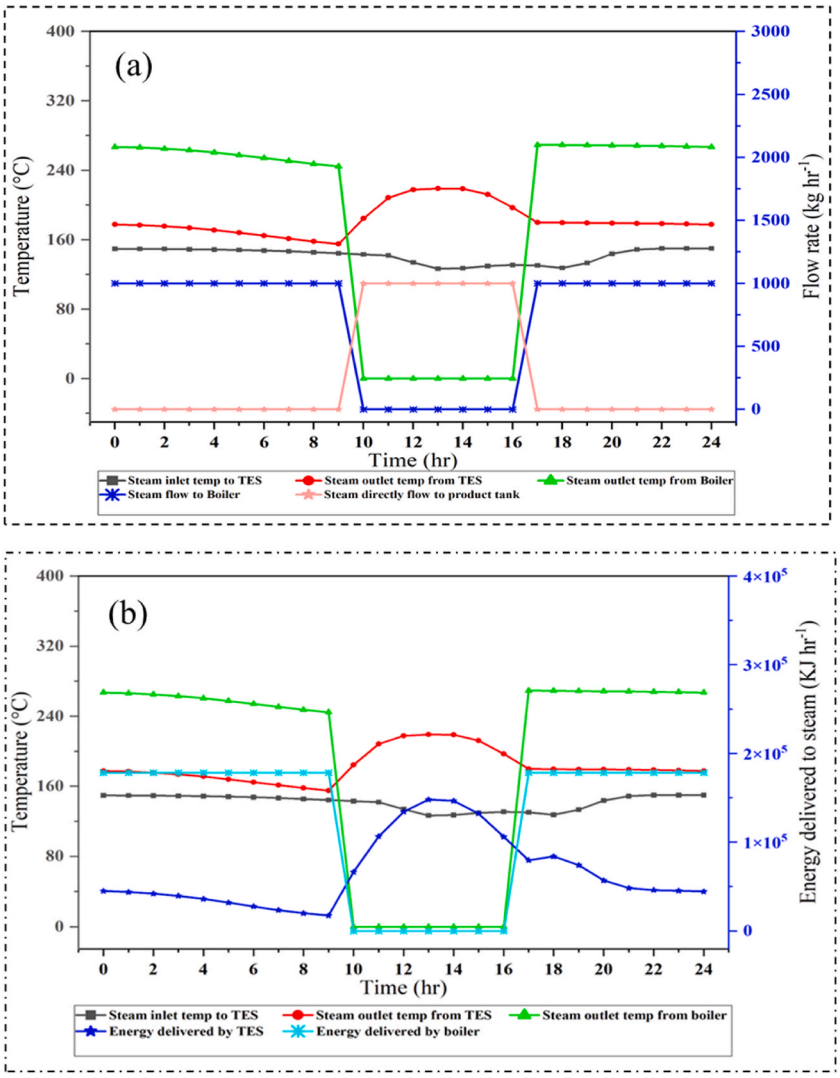

Fig. 6. (a) Steam temperature at the inlet and outlet of TES and boiler, outlet flow from diverter, on a sunny day (b) Steam inlet and outlet temperature at TES and boiler, energy delivered by TES and boiler to steam, on a sunny day.

steam loss energy, and again enter to TES tank for gaining thermal energy to repeat the cycle. But when the temperature of steam at the exit of TES or the inlet of the diverter is less than 180 °C, then the controller closed outlet 1 of the diverter and opens outlet 2 of the diverter. Outlet 2 of the diverter flows toward the boiler where conventional fuels burn to increase the temperature of steam. By gaining thermal energy from the boiler the steam flow to outlet 2 of the mixer and proceed to the product storage tank to maintain the temperature of the products. As shown in a diagram during the daytime the steam exit temperature from TES is greater than 180 °C whereas at night-time the steam temperature is less than 180 °C and steam flow toward the boiler while conventional fuels burn to increase the temperature of steam.

On a sunny day during the daytime solar energy is available, the TES tank stores abundant energy and delivered more energy to steam after passing from the TES tank, and energy delivered from the boiler is zero. The higher the temperature of the output steam from TES, the more significant the reduction in the boiler's overall fuel usage will be. While at night-time TES the tank is discharged by supplying energy to steam, but if energy delivered by TES to steam is not sufficient, then the required energy is delivered by the boiler as shown in Fig. 6(b).

During night-time, steam enter Tk-301 at the temperature of 235-225 °C, then flow towards Tk-328 to maintain the bitumen 2nd tank temperature at the temperature of 225-208 °C. After that steam flow toward RFO product storage tank Tk-307 at the temperature of 208-195 °C and Tk-5 inlet temperature of the steam is 180-170 °C and then enters to TES tank at temperature of 149-141 °C as shown in Fig. 7(a). From the figure, the temperature of steam after passing each storage tank falls by maintaining the temperature of products. At night-time, the steam temperature is higher as compared to the daytime on a sunny day. Because at night-time steam outlet temperature from the TES tank is less, therefore the boiler runs to increase the temperature of steam, while in daytime steam gain

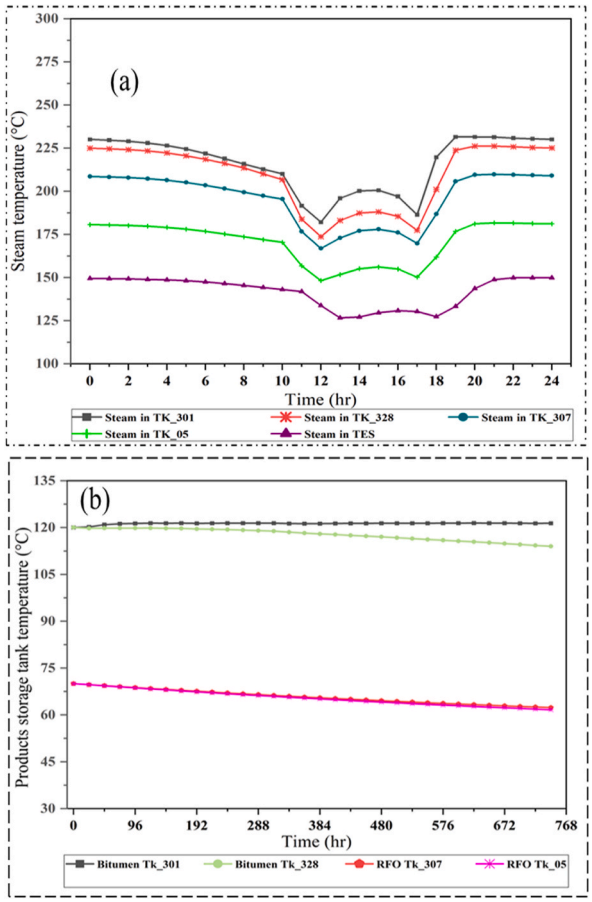

Fig. 7. (a) Temperature of steam at the inlet of the product storage tank and Thermal energy storage tank, on a sunny day (b) Monthly product storage tank temperature.

energy only from the TES tank, usually, the boiler does not run during the daytime on a sunny day. Products bitumen produced from the vacuum distillation tower and RFO from the atmospheric distillation tower in the refinery. Bitumen storage temperature is 110–120 °C in the winter and 100–110 °C in the summer. The storage temperature of RFO is 60–70 °C in the winter and 55–60 °C in the summer. When the temperature of these products in the storage tank falls below a certain point, condensate forms in the tank, causing an issue for dispatch. Fig. 7(b) shows the monthly storage temperature of bitumen at Tk-301, Tk-328, and RFO at Tk-307, Tk-05. The annual product storage tank temperature is shown in Fig. S5.

3.2. Thermal performance analysis on cloudy days

On certain days of the year, when the sky is overcast during specific hours of the day, radiation from the sun diminishes, resulting in a drop in the outflow temperature of HTF from the PTC as shown in Fig. 8(a). As a result, the change in the outlet temperature of HTF from the solar field will not charge the TES tank. Fig. 8(b) demonstrates that the nodes temperature of the TES tank on a cloudy day is not changed as compared to Fig. 5(b) nodes temperature of the TES tank on a sunny day.

On a cloudy day, the HTF used for the charging of TES tank has insufficient energy to charge the TES tank, therefore the steam inlet and outlet temperature at the TES tank is usually the same, and the outlet temperature of the steam is less than 180 °C, therefore diverter outlet 2 open to allow the fluid flow towards boiler where the steam gain thermal energy as shown in Fig. 9(a). The boiler reduction of fuel is less during the daytime on a cloudy day as compared to a sunny day. Fig. 9(b) demonstrates that energy delivered by boiler is high and TES is zero on cloudy day.

Thermal efficiency is one of the most significant factors to consider when evaluating the performance of a solar field with a PTC. The thermal efficiency of the collector is the ratio of thermal energy absorbed by the HTF to the flux of direct radiation that reached the collector, and it depends on several variables including the geometry of the solar collector, the temperature of the circulating HTF, and the surrounding temperature. Fig. S6 shows the thermal efficiency of the solar field throughout the year. Additionally, as the solar elevation angle in the sky falls (end losses), the radiation reflected by the reflector at the end of the collection will not be reflected on the absorbing pipe, reducing the collector's efficiency. The losses resulting from the end effect in this investigation are not substantial due to the low length of the rows of collectors. A rise in solar field HTF temperature or a decrease in air temperature frequently decreases the collector's thermal efficiency. This decrease in efficiency is caused by a greater thermal loss between the absorbing pipe

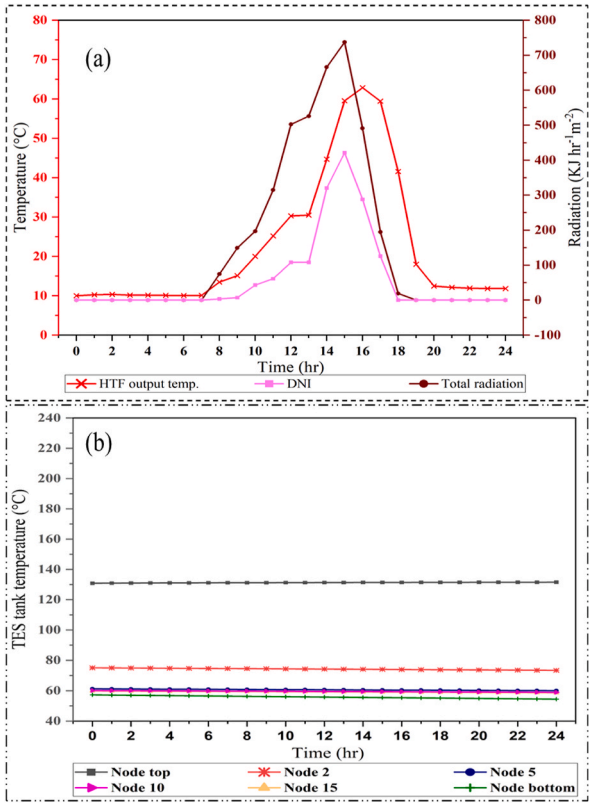

Fig. 8. (a) Temperatures at the solar collector output, total horizontal radiation, and DNI, on a cloudy day (b) TES tank node temperature, on a cloudy day.

and the surrounding air.

3.3. Fuel type analysis

The fuel system at the refinery is designed to ensure an adequate supply of fuel for refinery operations. This is accomplished with the use of solid fuel, liquid fuel, and gas fuel. Natural gas and liquefied petroleum gas (LPG) are the principal sources of input fuel gases to the boiler. Natural gas has a calorific value of 35.98 MJ/m^3 and LPG has 25.402 MJ/L [36]. The set value for the pressure of the gas in refinery use is 30 psi and for domestic use is 5–6 psi.

The furnace fuel oil system provides the necessary fuel oil to the plant and boiler house. Heavy oil (fuel oil), light diesel oil (LDO), and Gasoline are the main sources of input fuel oil for the boiler. The calorific value of heavy oil, LDO, and Gasoline is 41.003 MJ/L, 36.819 MJ/L, and 34.78 MJ/L respectively. The thermal efficiency of natural gas and LDO fired boiler is 85%, LPG and gasoline fired boilers is 80% and heavy oil fired boiler is 76% [36]. Fig. S7 shows the ideal and actual calorific values of different types of fuels used in the refinery boiler.

3.4. CO_2 emissions reductions and energy analysis

One of the significant gains of using solar collectors to fulfill the thermal requirements of the product storage tank in the refinery is the substantial reduction in emissions of GHG. In Fig. 10(a) the pink column reflects annual CO_2 emissions from the combustion of conventional fuel to generate steam, while the green column demonstrates that CO_2 emissions are decreased when steam is generated by a solar hybrid system. Natural gas and heavy oil are the most common fuels used to provide industrial process heat.

Most industries, including paper, fabric, PVC, chemical, and oil, run at temperatures of steam ranging from 120 °C to 220 °C, fulfilling the heat requirement [37,38]. In the present study, a steam temperature ranging from 180 °C to 220 °C is required for maintaining the temperature of heavy crude oil refinery products in storage tanks before despatch. For such a temperature range of steam, approximately 1.5592E+09 kJ of energy is consumed annually from conventional fuel. With hybrid system integration, the annual energy consumption of the boiler was decreased to 1.15E+09 kJ while the remaining energy 4.21E+08 kJ was supplied by the solar system. The energy consumption of the auxiliary boiler and the amount of energy delivered by TES to steam is shown in Fig. 10 (b). From the figure, the energy delivered to process steam by boiler is reduced due to hybrid system integration. Because due to sunny day the steam gains thermal energy from TES while on a cloudy day or when TES fully discharged then the boiler runs for generation of steam.

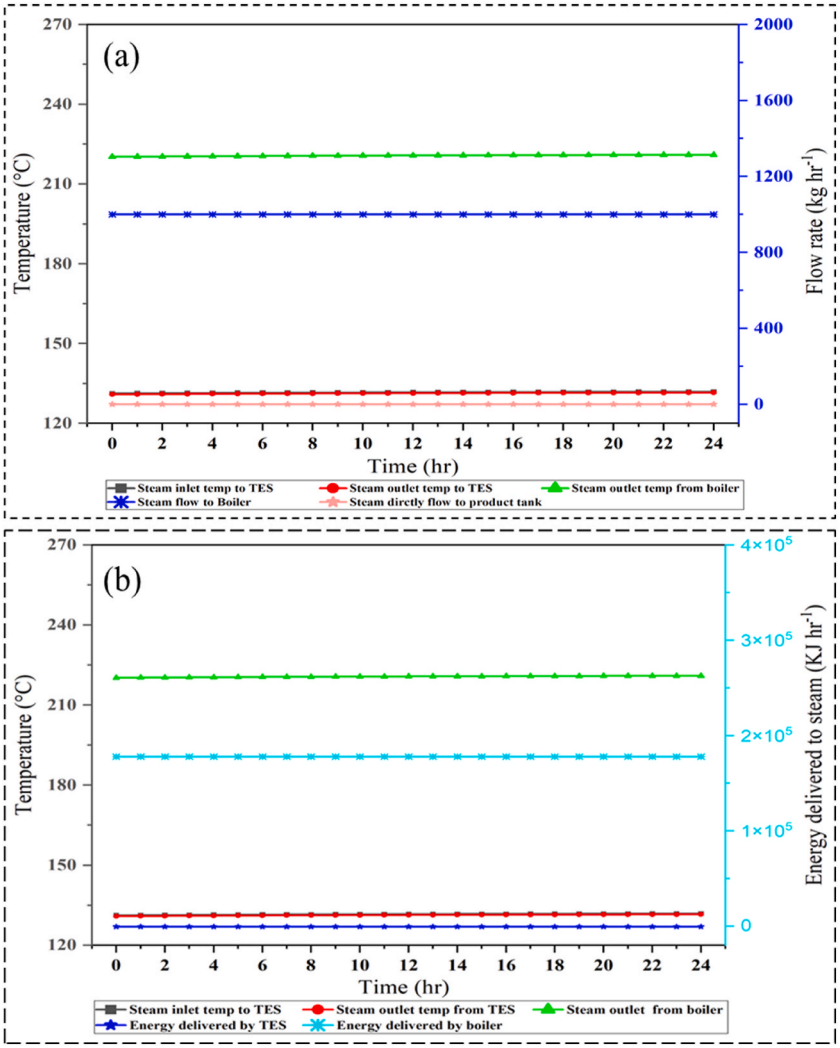

Fig. 9. (a) Steam temperature at the inlet and outlet of TES and boiler, outlet flow from diverter, on a cloudy day (b) Steam inlet and outlet temperature at TES and boiler, energy delivered by TES and boiler to steam, during a cloudy day.

3.5. Cost analysis for a solar hybrid heavy product storage system

One of the most important steps in performing an economic analysis of a project is determining the costs, including the costs of necessary equipment. The costs in this study can be divided into two categories: initial costs and annual costs are shown in Table 4. Initial expenses can be subdivided into direct and indirect expenses. Direct cost consists of the cost of the collector, pump, pipe, heat exchanger, thermal storage tank, diverter, and ground preparation.

The obtained information is then used to find the payback period of the system. Eq. (10) is used for calculating the payback period system.

$$\text{Payback period} = \frac{\text{Capital cost of the system}}{\text{Average annual cash inflow}} \tag{10b}$$

For payback time calculation, overall investment and yearly cash return or inflows are required, the overall investment is determined by adding the cost of all components and yearly Operation and Maintenance (O&M) expenses. Annual O&M costs are equal to 0.75% of the initial investment [52]. The total cost for the proposed system is shown in Table 5.

The average price of natural gas is 0.78128$/m^3, LPG is 0.77$/litre, heavy oil is 1.46$/litre, Light Diesel oil is 1.38$/litre and gasoline is 1.41$/litre [53]. The amount of fuel and cost savings by the integration of a solar hybrid system into the refinery and the payback period of the system by using different types of fuel in the furnace are shown in Table 6.

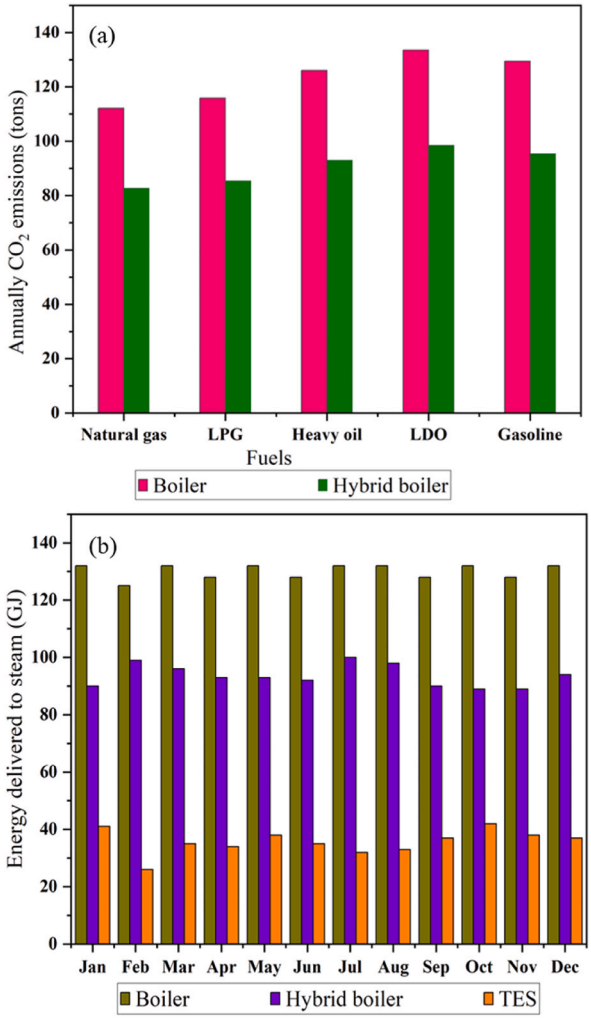

Fig. 10. (a) Annually CO_2 emission by burning of different fuels in Refinery boiler (b) Energy delivered to steam by the auxiliary boiler, hybrid boiler, and TES.

Table 4
Initial component costs.

Equipment/Job	Quantity/size	Cost Per Unit ($)	Total cost ($)
Direct cost			
Parabolic Trough collector	463m^2	270/m^2 [39,40]	125,010
Ground preparation cost (5.7% of the collector cost) [41]			7125.57
Pumps	3	700-800/each [42–44]	2100_2400
Piping	1400 m	0.80-0.84/m [45,46]	1120_1200
Thermal storage tank	15m^3	1060/m^3 [33]	15,900
Heat exchanger	1	4000/each [47]	4000
Diverter	1	600/each [48,49]	600
Total direct cost			156,235.57
Indirect cost			
Engineering, construction, and ownership (10% 0f direct cost) [50]			15,623.557
Total investment cost [51]	Direct + indirect cost		171,859.127

Table 5
Proposed system cost.

Technology	Initial cost ($)	Annual O&M ($)	Total cost ($)
PTC	171,859.127	1288.943	173,148.07

Table 6
Payback period of the proposed system by using different fuel.

Fuel	Fuel saving	Cost saving	Payback period
Natural gas	13,765.817 m^3	10,754.957$	16.09 years
LPG	20,717.484 L	15,952.462$	10.85 years
Heavy oil	13,510.044 L	19,724.664$	8.77 years
LDO	13,452.198 L	18,564.033$	9.32 years
Gasoline	15,130.822 L	21,334.459$	8.11 years

4. Conclusion

The present study investigates the feasibility of solar hybrid system to generate steam in the oil refinery to maintain the temperature of heavy crude oil products before despatching from storage tanks. Due to the intermittent behaviour of solar energy, the solar hybrid system is integrated with a sensible heat storage tank. The suggested hybrid solar heating system for the refinery was simulated using TRNSYS software, followed by experimental validation. The main conclusions from this study are summarized as follows:

- The energy required from boiler to produce steam is decreased when a solar system coupled with TES is added.
- The effect of ambient temperature on PTC outlet temperature was investigated and it was observed the amount of fuel needed for steam in boilers decreased by 31.50% on sunny days because of energy gain of 1.52E+06 kJ from TES.
- On cloudy days, when the TES is not fully charged, the steam receives just 4.02E+05 kJ of thermal energy from the TES, which is a relatively little quantity, resulting in a boiler that supplies 88.74% of the energy required.
- Solar energy may contribute a maximum of 26.99% of the boiler's annual energy consumption under optimal conditions. This reduces the boiler's use of heavy fuel oil by 13510.044 L and prevents the unit boiler from generating 34.045 tonnes of carbon dioxide annually.

This reduction in fuel consumption and carbon dioxide emissions is exclusive to one boiler (ton/day steam) of the refinery, but it may be extended to the other boilers to gain significant fuel savings and GHG reduction. Due to global environmental concerns, this study tends to contribute towards lowering GHG emissions and reducing fossil fuel consumption in the crude oil refinery industry, which is among the most fuel intensive industries.

Credit authors statement

Conceptualization; A.H.K and N.A, Data curation; N.A and N.A.K.
Formal analysis; M.A.M and N.A.
Funding acquisition; F.R.
Investigation; N.A, A.H.K and N.A.K.
Methodology; N.A.K and M.M.
Project administration; A.H.K, F.R and M.A.
Resources; M.A, N.A and A.H.K.
Software; M.M, N.A and N.A.K.
Supervision; A.H.K and N.A.
Validation; M.A.M and M.A.K.
Visualization; M.M and M.A.M.
Writing - original draft; A.H.K, N.A and N.A.K.
Writing - review & editing: F.R, M.A and M.A.K.

Declaration of competing interest

There is no conflict of interest.

Data availability

No data was used for the research described in the article.

Acknowledgements

This work has been partially funded by Abu Dhabi University, UAE.

Appendix A. Supplementary data

Supplementary data to this article can be found online at https://doi.org/10.1016/j.csite.2023.103276.

References

[1] A. Szklo, R. Schaeffer, Fuel specification, energy consumption and CO2 emission in oil refineries, Energy 32 (7) (2007) 1075–1092.
[2] L. Kumar, M. Hasanuzzaman, N. Rahim, Global advancement of solar thermal energy technologies for industrial process heat and its future prospects: a review, Energy Convers. Manag. 195 (2019) 885–908.
[3] F. Perera, K. Nadeau, Climate change, fossil-fuel pollution, and children's health, N. Engl. J. Med. 386 (24) (2022) 2303–2314.
[4] J. Luoma, The Challenge for Green Energy: How to Store Excess Electricity, Guardian Environment Network. The Guardian, 2009.
[5] D. Gao, J. Li, X. Ren, T. Hu, G. Pei, A novel direct steam generation system based on the high-vacuum insulated flat plate solar collector, Renew. Energy 197 (2022) 966–977.
[6] A. Rafiee, K.R. Khalilpour, Renewable hybridization of oil and gas supply chains, in: Polygeneration with Polystorage for Chemical and Energy Hubs, Elsevier, 2019, pp. 331–372.
[7] A. Sandá, S.L. Moya, L. Valenzuela, Modelling and simulation tools for direct steam generation in parabolic-trough solar collectors: a review, Renewable Sustainable Energy Rev. 113 (2019), 109226.
[8] A.K. Sharma, C. Sharma, S.C. Mullick, T.C. Kandpal, Carbon mitigation potential of solar industrial process heating: paper industry in India, J. Clean. Prod. 112 (2016) 1683–1691.
[9] B. Stanek, D. Węcel, Ł. Bartela, S. Rulik, Solar tracker error impact on linear absorbers efficiency in parabolic trough collector–Optical and thermodynamic study, Renew. Energy 196 (2022) 598–609.
[10] Y.-L. He, et al., Perspective of concentrating solar power, Energy 198 (2020), 117373.
[11] Z. Li, et al., Applications and technological challenges for heat recovery, storage and utilisation with latent thermal energy storage, Appl. Energy 283 (2021), 116277.
[12] B. Koçak, A.I. Fernandez, H. Paksoy, Review on sensible thermal energy storage for industrial solar applications and sustainability aspects, Sol. Energy 209 (2020) 135–169.
[13] H. Jouhara, A. Żabnieńska-Góra, N. Khordehgah, D. Ahmad, T. Lipinski, Latent thermal energy storage technologies and applications: a review, International Journal of Thermofluids 5 (2020), 100039.
[14] O. Siddiqui, I. Dincer, Analysis and performance assessment of a new solar-based multigeneration system integrated with ammonia fuel cell and solid oxide fuel cell-gas turbine combined cycle, J. Power Sources 370 (2017) 138–154.
[15] M. Ezzat, I. Dincer, Energy and exergy analyses of a new geothermal–solar energy based system, Sol. Energy 134 (2016) 95–106.
[16] A.K. Sharma, C. Sharma, S.C. Mullick, T.C. Kandpal, Potential of solar industrial process heating in dairy industry in India and consequent carbon mitigation, J. Clean. Prod. 140 (2017) 714–724.
[17] A. Baniassadi, M. Momen, M. Amidpour, O. Pourali, Modeling and design of solar heat integration in process industries with heat storage, J. Clean. Prod. 170 (2018) 522–534.
[18] A. Allouhi, et al., Design optimization of a multi-temperature solar thermal heating system for an industrial process, Appl. Energy 206 (2017) 382–392.
[19] B. Mokhtari Shahdost, M.A. Jokar, F. Razi Astaraei, M.H. Ahmadi, Modeling and economic analysis of a parabolic trough solar collector used in order to preheat the process fluid of furnaces in a refinery (case study: parsian Gas Refinery), J. Therm. Anal. Calorim. 137 (2019) 2081–2097.
[20] K. Altayib, I. Dincer, Analysis and assessment of using an integrated solar energy based system in crude oil refinery, Appl. Therm. Eng. 159 (2019), 113799.
[21] B.C. Assis, et al., Constrained thermohydraulic optimization of the flow rate distribution in crude preheat trains, Chem. Eng. Res. Des. 91 (8) (2013) 1517–1526.
[22] E. Ishiyama, A. Heins, W. Paterson, L. Spinelli, D. Wilson, Scheduling cleaning in a crude oil preheat train subject to fouling: incorporating desalter control, Appl. Therm. Eng. 30 (13) (2010) 1852–1862.
[23] M. Al-Otaibi, A. Elkamel, T. Al-Sahhaf, A. Ahmed, Experimental investigation of crude oil desalting and dehydration, Chem. Eng. Commun. 190 (1) (2003) 65–82.
[24] L. Valenzuela, E. Zarza, M. Berenguel, E.F. Camacho, Control concepts for direct steam generation in parabolic troughs, Sol. Energy 78 (2) (2005) 301–311.
[25] M. Ghodbane, et al., Thermal performance assessment of an ejector air-conditioning system with parabolic trough collector using R718 as a refrigerant: a case study in Algerian desert region, Sustain. Energy Technol. Assessments 53 (2022), 102513.
[26] K. Mohammadi, S. Khanmohammadi, J. Immonen, K.J.S.E.T. Powell, Assessments, Techno-economic Analysis and Environmental Benefits of Solar Industrial Process Heating Based on Parabolic Trough Collectors, vol. 47, 2021, 101412.
[27] K. Mohammadi, S. Khanmohammadi, J. Immonen, K. Powell, Techno-economic analysis and environmental benefits of solar industrial process heating based on parabolic trough collectors, Sustain. Energy Technol. Assessments 47 (2021), 101412.
[28] Y. Krishna, M. Faizal, R. Saidur, P. Manihalla, S. Karinka, Performance analysis of Parabolic Trough Collector using TRNSYS®-A case study in Indian coastal region, J. Phys. Conf. 1921 (1) (2021), 012063. IOP Publishing.
[29] W.A.D. Beckman, Solar Engineering of Thermal Processes, 2010.
[30] H.M. Ushamah, et al., Techno-economic analysis of a hybrid district heating with borehole thermal storage for various solar collectors and climate zones in Pakistan, Renew. Energy 199 (2022) 1639–1656.
[31] A. Mawire, Performance of Sunflower Oil as a sensible heat storage medium for domestic applications, J. Energy Storage 5 (2016) 1–9.
[32] S. Nakul, U. Arunachala, Stability and thermal analysis of a single-phase natural circulation looped parabolic trough receiver, Sustain. Energy Technol. Assessments 52 (2022), 102242.
[33] A. Allouhi, et al., Design Optimization of a Multi-Temperature Solar Thermal Heating System for an Industrial Process, vol. 206, 2017, pp. 382–392.
[34] D.B. Fox, D. Sutter, J.W. Tester, The thermal spectrum of low-temperature energy use in the United States, Energy Environ. Sci. 4 (10) (2011) 3731–3740.
[35] H. Heubaum, F. Biermann, Integrating global energy and climate governance: the changing role of the International Energy Agency, Energy Pol. 87 (2015) 229–239.
[36] K.R. Kumar, N.K. Chaitanya, N.S. Kumar, Solar thermal energy technologies and its applications for process heating and power generation–A review, J. Clean. Prod. 282 (2021), 125296.
[37] D.B. Fox, D. Sutter, J.W.J.E. Tester, E. Science, The Thermal Spectrum of Low-Temperature Energy Use in the United States, vol. 4, 2011, pp. 3731–3740, 10.
[38] H. Heubaum, F.J.E.P. Biermann, Integrating Global Energy and Climate Governance: the Changing Role of the, vol. 87, International Energy Agency, 2015, pp. 229–239.
[39] L. Kumar, M. Hasanuzzaman, N. J. E. C. Rahim, and Management, Global Advancement of Solar Thermal Energy Technologies for Industrial Process Heat and its Future Prospects: A Review, vol. 195, 2019, pp. 885–908.
[40] K.R. Kumar, N.K. Chaitanya, N. S. J. J. o. C. P. Kumar, Solar Thermal Energy Technologies and its Applications for Process Heating and Power Generation–A Review, vol. 282, 2021, 125296.
[41] B. Mokhtari Shahdost, M.A. Jokar, F. Razi Astaraei, M. H. J. J. o. T. A. Ahmadi, and Calorimetry, Modeling and Economic Analysis of a Parabolic Trough Solar Collector Used in Order to Preheat the Process Fluid of Furnaces in a Refinery (Case Study: Parsian Gas Refinery), vol. 137, 2019, pp. 2081–2097, 6.
[42] I. P. W. C. W. p, A. from [Online]. Available: https://ironpump.com.
[43] L. P. P. G. A. f, Shanghai pacific pump manufacture (group) Co. [Online]. Available: https://www.pacific-pump-china.com/pump/centrifugal-pump/.
[44] S. P. Online, SuppliersPlanet, Uttar Pradesh India [Online]. Available: https://www.supplierspla net.com/diverter-valve.
[45] L. P. P. A. c. O. a, August 2022. [Online]. Available: https://www.alibaba.com/trade/search?spm=a2700.searchcustom.0.0.555f6f63N2VjLO&IndexArea=product_en&SearchText=pvc_pipes&f0=y.
[46] l. P. R. A. f., Shanghai ruihe enterprise group Co., Available: https://www.rehomepipe.com/.
[47] H. E. V. O. A. A. f., heat-exchangers.uk/pricelist." [Online]. Available: https://www.heat-exchangers.uk/pricelist.
[48] D.V. Price, Connecting buyers with Chinese suppliers [Online]. Available: https://www.made-in-china.com/products-search/hot-china-products/Diverter_Valve_Price.html.

[49] P. list, Hayward flow control [Online]. Available: https://www.haywardflowcontrol.com/en_us/price-lists.
[50] P. Kurup, C. Turchi, Initial Investigation into the Potential of CSP Industrial Process Heat for the Southwest United States, National Renewable Energy Lab. (NREL), Golden, CO (United States), 2015.
[51] K. Mohammadi, S. Khanmohammadi, H. Khorasanizadeh, K.J.S.E.T. Powell, Assessments, Development of High Concentration Photovoltaics (HCPV) Power Plants in the US Southwest: Economic Assessment and Sensitivity Analysis, vol. 42, 2020, 100873.
[52] J. R. J. G. E. N. T. G. Luoma, The Challenge for Green Energy: How to Store Excess Electricity, 2009.
[53] Online, Global petrol prices [Online]. Available: https://www.globalpetrolprices.com.